

COMPARISON OF SGLI AND MODIS DERIVED LAND SURFACE TEMPERATURE FOR AGRICULTURAL MONITORING

Tatsuyuki Sagawa (1), Kei Oyoshi (1), Yoshinobu Sasaki (1), Hiroshi Murakami (1)

¹Earth Observation Research Center, Japan Aerospace Exploration Agency, 2-1-1 Sengen, Tsukuba, Ibaraki 305-8505, Japan

Email: sagawa.tatsuyuki@jaxa.jp; ohyoshi.kei@jaxa.jp; sasaki.yoshinobu@jaxa.jp; murakami.hiroshi.eo@jaxa.jp

KEY WORDS: SGLI, GCOM-C, MODIS, land surface temperature, drought

ABSTRACT: Land surface temperature (LST) products derived by Second-generation Global Imager (SGLI) onboard the Global Change Observation Mission-Climate (GCOM-C) satellite are provided by Japan Aerospace Exploration Agency (JAXA). GCOM-C was launched on 23 December 2017 and LST data is available from January 2018 with 250m or 1/24 degree spatial resolution. LST is used for various purposes and drought detection as agro-meteorological information is one of them. Drought event is detectable using anomaly value by comparing observation value and normal year value. However, normal year value should be calculated from long term data and SGLI does not yet have long term data storage. Moderate Resolution Imaging Spectroradiometer (MODIS) onboard Terra and Aqua satellites have also contributed for LST observation and have long term data storage. Thus, normal year value derived by MODIS may be applicable for anomaly calculation for SGLI data. In this study, SGLI L3 LST and MOD11C1 half month composite images were compared in 5 regions from 2018 to 2019 to examine the compatibility of these two products. Time series trend of the anomaly data from SGLI L3 LST and MOD11C1 was similar in Thailand, although anomaly was only slightly high during the drought event. It indicates anomaly of SGLI L3 LST using MOD11C1 normal year value could be used to detect extreme events as same as anomaly of MOD11C1.

1. INTRODUCTION

World population is forecasted to reach 9 billion in 2050 and 70 % increase of food supply will be required (FAO, 2009). Stable food supply through sustainable agriculture has become important given the limited resources. Decision makers should make plans for sustainable and stable food supply based on accurate information about yield to address climate change impact on agriculture and continuous increase in the consumption due to population growth. Thus, accurate and efficient method is required for yield estimation.

Satellite derived information such as land surface temperature (LST), precipitation, drought index are useful as agro-meteorological (agromet) information. If there are long time archives of these data, they can be used to detect, make counter measures and probably predict important calamities such as drought. A drought or a flood event can be detected as an anomaly value by comparing agromet data with normal year data. Normal year agromet data can be created by averaging data collected over a longtime. This study was focused on LST data, which is one of the main contributing factor to a drought.

Global Change Observation Mission-Climate (GCOM-C) satellite launched by JAXA on 23 December 2017 has the Second-generation Global Imager (SGLI) payload which has bands capable to estimate LST. To detect drought events using LST, anomaly value calculated as difference between target LST and normal year LST is useful. However, GCOM-C has data stacks for less than 3 years and duration of data is not enough to calculate typical normal year LST value. Terra and Aqua are NASA's satellites those have Moderate Resolution Imaging Spectroradiometer (MODIS) payloads which also has bands for LST estimation. Terra was launched on 18 December 1999 and Aqua was launched on 4 March 2002, respectively. Thus, there are data stacks of MODIS for more than 20 years can be considered as longtime observation sufficient to derive normal year LST. Based

on this MODIS normal year LST, LST anomaly of SGLI could be calculated. Then, to confirm the compatibility between LST from SGLI and MODIS, agroclimatic products of both the sensors were compared. The effectiveness and suitability of LST anomaly of SGLI using MODIS based normal year LST was investigated for drought detection.

2. DATA AND STUDY AREA

SGLI Level-3 daily LST product with the spatial resolutions of 1/24 degrees was used for the analysis in this study. GCOM-C is placed in an orbit to cross the equator at 10:30 am local time. On the other hand, Terra and Aqua satellites are placed to cross the equator at 10:30 am and 1:30 pm local time, respectively. Given the similar observation time of Terra/MODIS with GCOM-C/SGLI, it can be assumed that the observation conditions of these two sensors would be very close to each other allowing simple comparison without adjusting to any observation parameters. MOD11C1 with 0.05 degree spatial resolution was selected as MODIS daily LST product.

JAXA developed the JAXA’s Satellite based MonItoring Network system (JASMIN) and provides the data service to the public. JASMIN system provides agro-meteorological products derived from satellite data every half month and these products include precipitation, drought index, soil moisture, radiation, NDVI and LST. Products derived from SGLI are also expected to be used in this system. In this study, we created half month composite images from LST daily data for comparison following flows in Figure 1.

SGLI data exist from January 2018 but data for first three months were not suitable for the analysis due to many missing values in the data. Therefore, SGLI and Terra/MODIS data from April 2018 to December 2019 were used for this study. SGLI data is resampled to adjust the spatial resolution of MOD11C1 and bilinear interpolation is applied as resampling method.

Climate Change Initiative (CCI) land cover provided by ESA was used to extract crop land area. This map classifies land types into 22 classes based on United Nations Food and Agriculture Organization’s (UN FAO) Land Cover Classification System (LCCS). Spatial resolution of this data is 300 meters and annual updates are available since 1992. The published map of 2018 was used as most recent data to match with satellite observations time period. This land cover map too was resampled to the spatial resolution of MOD11C1 for easy comparisons. During the re-sampling, the crop coverage ratio was calculated for each pixel and a pixel with more than 50 % crop coverage is extracted as a crop pixel.

Five comparison regions (Japan, China, India, South East Asia 1 and South East Asia 2) were selected in Asia as shown in Figure 2. In these regions, rice field is widely distributed and damage for crops have been often reported due to severe drought or flood events. In June 2019, severe drought was reported in Thailand and detail survey was conducted for drought detection using LST data.

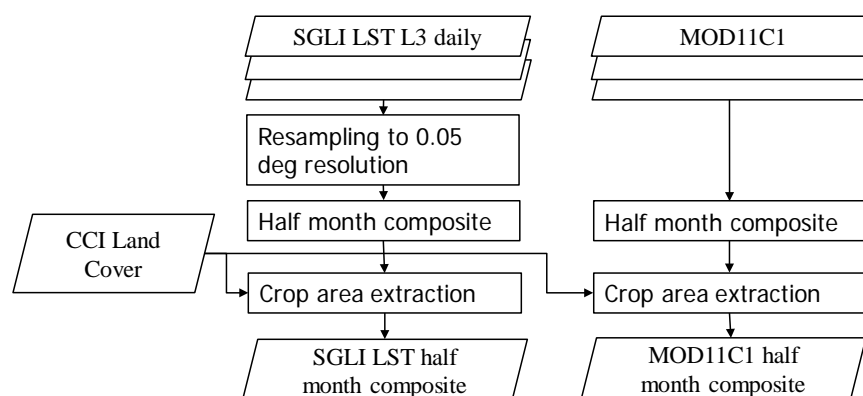


Figure 1 Creation of half month composite images

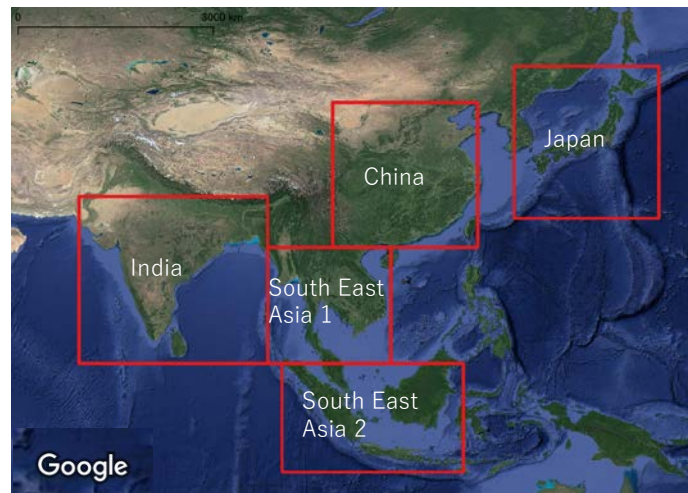


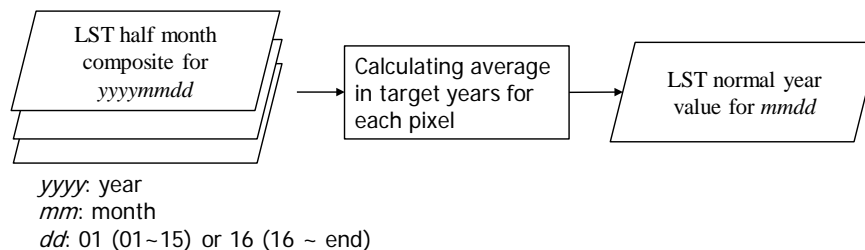
Figure 2 Comparison regions

3. METHOD

Half month composite LST images were created from SGLI L3 daily LST data and MOD11C1, respectively. Each pixel value in the composite image is the average LST of a half month period. Normal year image was created averaging long years of data for the same half month period (Step1 in Figure 3). In the Figure 3, the date is expressed to show the data aggregation for half-months expressing the first half month as $yyyymm01$ and the second half month as $yyyymm16$. Where, $yyyy$ is year and mm is month, respectively. Having completed these sets of spatial and temporal compatible composites, the anomaly image was created taking the difference between both LST image composites (Step 2 in Figure 3). The resulted anomaly image represented the deviation of 2018 LST from a normal year. Obtaining anomaly value for SGLI using MODIS normal year value is objective in this study.

Each crop area pixel values in LST images, normal year images and anomaly images derived from SGLI L3 LST and MOD11C1 were compared. Considering MOD11C1 as true data, root mean square error (RMSE) and mean bias error (MBE) were calculated in target regions for each SGLI derived data. In China and India regions, number of data in a scene was large. Therefore, 10,000 data points were randomly sampled in these two regions when number of data exceeded 10,000. Detection of drought event in Thailand was also investigated using these data.

Step1. Calculation of normal year value



Step1. Calculation of anomaly value

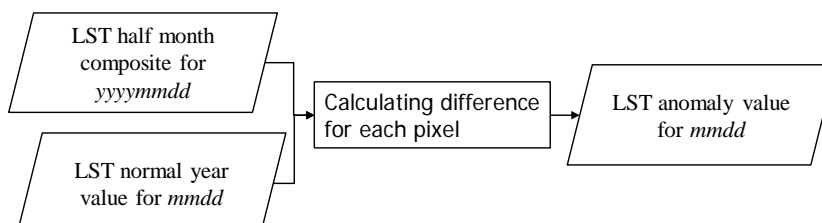


Figure 3 Calculation of normal year and anomaly values

4. RESULTS AND DISCUSSION

Figure 4 shows LST scatter plots for 5 comparison regions for the first half of April 2018. Temperature range, RMSE and MBE are largely different among regions. Table 1 summarizes comparison results for target duration. In the table, the units of RMSE and MBE are Kelvin. The date is expressed to show the data aggregation as same as defined in Figure 3. Maximum RMSE, maximum MBE and minimum MBE are 9.70 K, 8.89 K and -7.42 K, respectively.

According to Moriyama (2020), MBE and RMSE of SGLI LST validated with ground truth data in USA and Canada flux sites are 2.36 K and 0.47 K, respectively. Wan (2014) reported the mean LST error of MODIS C6 level-2 LST is within ± 0.6 K in 10 validate data sets. When compared with these validation works, the differences between SGLI LST and MOD11C1 from our results are considerably large.

To cover the selected target regions in Figure 2, it was necessary to acquire both MODIS and GCOM-C images observed from multiple orbits. Because of this reason, there is a difference in the observation time between SGLI L3 LST and MOD11C1 images in some target regions. In extreme cases, the observation time difference was over 2 hours. Though it is not quantitatively analyzed, it could be said that this time difference may have contributed to the significant difference between SGLI L3 LST and MOD11C1 LST.

Anomaly images calculated using normal year data from 2018 to 2019 for Thailand in second half month of July 2019 is shown in Figure 5. In Figure 5, anomaly is expressed with range of ± 10 K. Although the anomaly is slightly positive in some regions, 2 years of data for calculation of normal year value may be not enough to further explore the reasons for the anomaly.

Figure 6 also shows anomaly images for Thailand in second half month of July 2019 but MOD11C1 data from 2009 to 2019 are used to calculate normal year value for both SGLI L3 LST and MOD11C1 anomaly. In Figure 4, both SGLI L3 LST and MOD11C1 anomaly are high in the central Thailand.

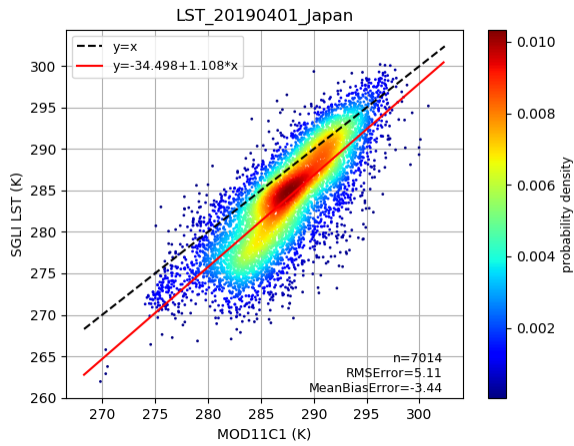
Figure 7 is the time series graph of spatial average of the 2019 LST anomaly in the central Thailand. MOD11C1 data from 2009 to 2019 were used to calculate normal year value. Although MOD11C1 anomaly in July is positive (1 to 2 K) it is not significant enough to conclude as a drought event. Anomaly of SGLI L3 LST are relatively higher than MOD11C1 but shows similar trend for time series changes. It means anomaly of SGLI L3 LST using MOD11C1 normal year value could be used to detect extreme events as same as anomaly of MOD11C1.

In this study LST was focused on to simplify the comparison between SGLI and MODIS products but concerning agriculture drought detection, normalized vegetation index (NDVI) is also useful (Sruthi and Aslam, 2015). It could be said that a comparison of the combination of both LST and NDVI from SGLI and MODIS is worth considering in the next step for better results.

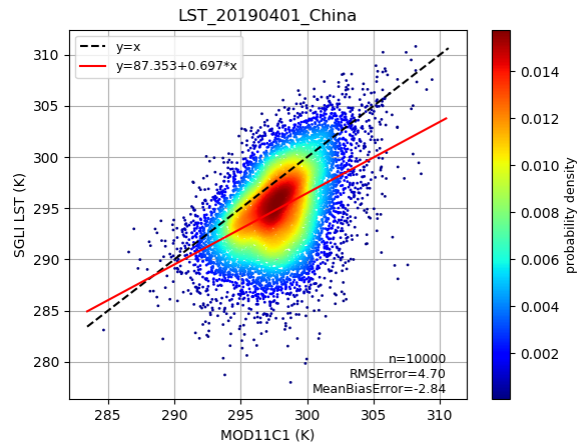
5. CONCLUSION

SGLI L3 LST and MOD11C1 half month composite images were compared in 5 regions from 2018 to 2019 and medians of RMSE were 3.95 to 5.33 K and medians of MBE were -1.92 to 2.07 K. Time series trend of the anomaly data from SGLI L3 LST and MOD11C1 was similar in Thailand. It indicates anomaly of SGLI L3 LST using MOD11C1 normal year value could be used to detect extreme events as same as anomaly of MOD11C1.

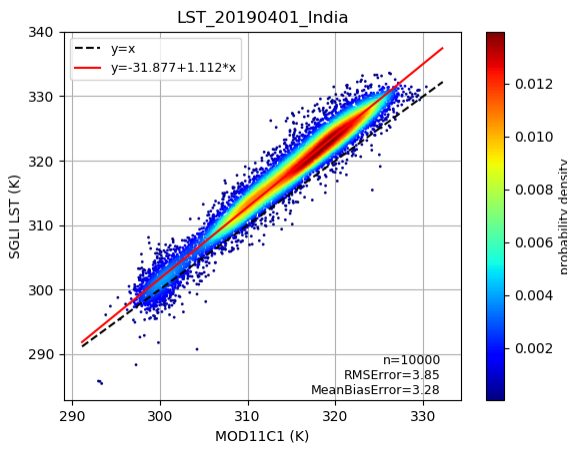
Further study with additional agromet events could help to deepen our understanding and improve reliability of the results. The research work will be continued with additional observation, covering more extreme events and it is expected to contribute to accurate and efficient monitoring of agromet events and crop outlook.



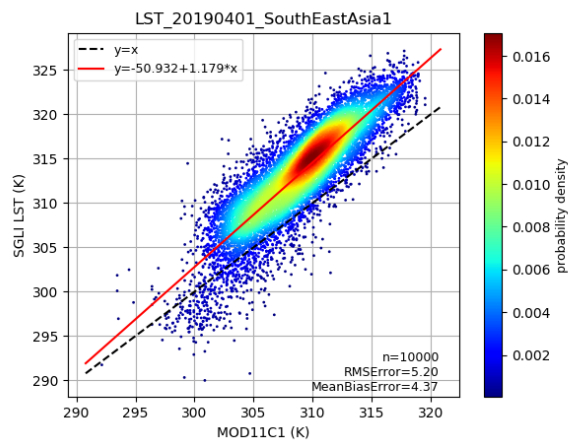
(a) Japan



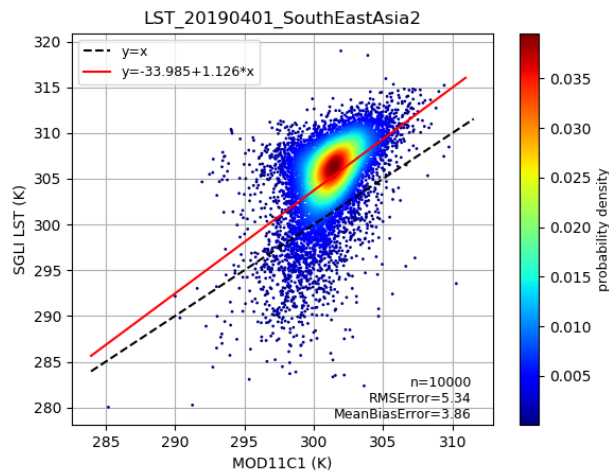
(b) China



(c) India



(d) South East Asia 1

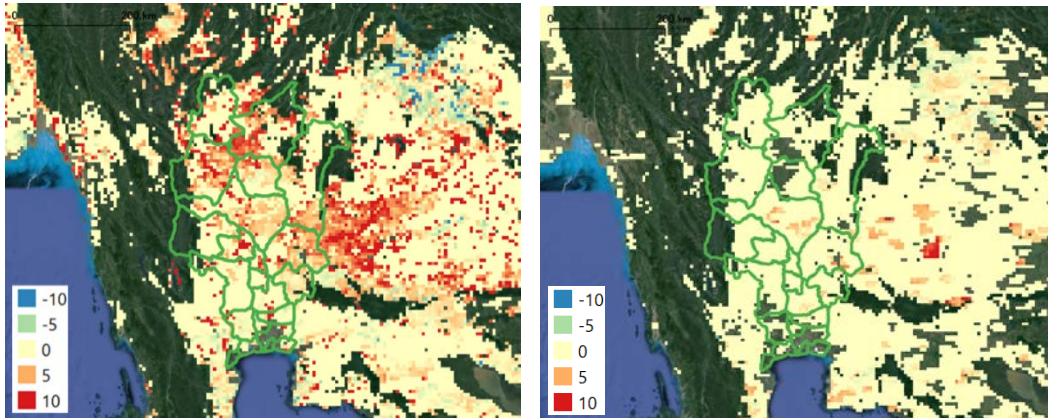


(e) South East Asia 2

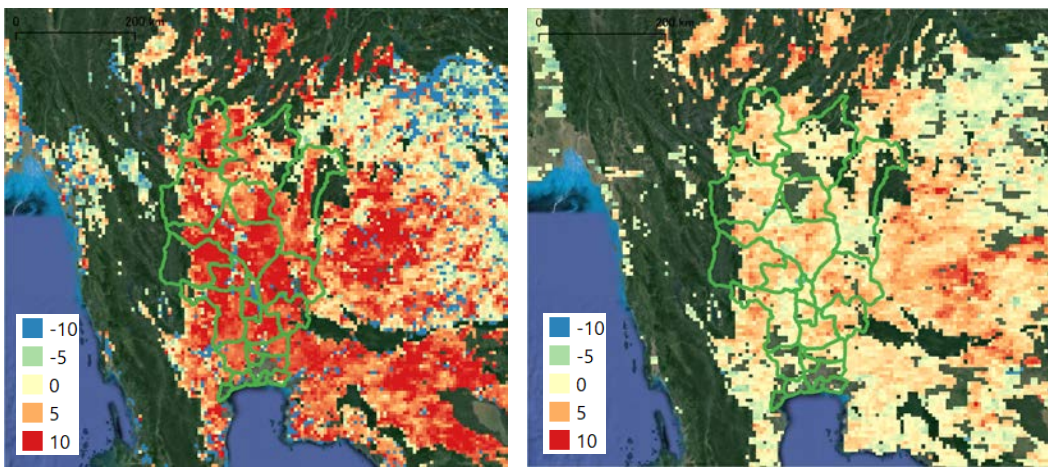
Figure 4 LST scatter plots for 5 regions for first half month of April 2018

Table 1 Summary for LST comparison results

	Japan		China		India		South East Asia 1		South East Asia 2	
Date	RMSE	MBE	RMSE	MBE	RMSE	MBE	RMSE	MBE	RMSE	MBE
20180401	4.64	-2.98	4.13	-2.31	3.79	3.23	3.78	2.74	4.55	2.34
20180416	3.20	-0.44	3.67	-0.83	4.42	3.69	4.53	2.83	5.01	2.58
20180501	5.13	-3.17	5.00	-1.04	4.60	3.72	5.10	3.61	4.10	2.53
20180516	3.92	-0.92	5.89	-1.80	5.65	4.63	5.67	3.33	5.36	1.78
20180601	4.44	-2.30	4.26	-0.79	5.28	2.32	8.72	0.61	4.13	2.17
20180616	4.25	-1.65	5.23	0.05	4.91	1.63	6.89	1.58	5.32	1.19
20180701	5.01	-0.47	4.51	0.03	6.31	0.85	6.13	1.13	4.43	1.30
20180716	3.98	1.68	4.33	1.69	7.25	-0.47	9.70	0.15	4.00	1.76
20180801	3.89	0.09	3.97	1.40	6.93	-1.52	7.48	0.06	3.83	1.54
20180816	4.65	-1.85	3.20	0.39	6.83	-0.91	7.59	-0.56	3.71	1.91
20180901	4.77	-2.47	4.14	-1.01	3.97	0.84	5.45	1.24	4.99	1.49
20180916	3.46	-1.44	4.78	-2.02	3.71	2.56	4.20	2.49	4.28	2.31
20181001	3.53	-1.95	4.21	-1.83	3.14	1.81	4.22	2.25	5.24	1.32
20181016	4.71	-3.18	4.67	-2.64	2.55	1.77	3.61	2.08	4.70	2.84
20181101	3.82	-2.98	6.91	-5.53	2.33	1.32	4.11	1.26	6.87	1.87
20181116	3.82	-2.59	4.89	-3.65	1.99	0.76	4.20	2.07	5.67	3.39
20181201	4.13	-2.38	8.30	-6.30	1.82	-0.09	4.39	0.89	6.68	2.31
20181216	3.51	-2.49	8.89	-7.24	1.80	-0.18	3.91	0.45	6.79	2.20
20190401	5.11	-3.44	4.64	-2.83	3.86	3.25	5.20	4.36	5.33	3.80
20190416	4.62	-2.33	5.22	-3.22	4.36	3.79	5.72	4.97	6.02	2.53
20190501	3.65	0.09	5.06	-2.23	4.43	3.80	5.57	2.88	5.00	3.95
20190516	3.56	-0.39	4.13	-1.65	4.85	4.40	5.90	3.91	4.86	3.19
20190601	4.73	-1.90	3.80	0.66	6.31	5.21	6.80	3.78	5.52	2.44
20190616	3.68	-1.15	5.19	0.35	5.48	2.72	6.69	1.87	4.35	1.97
20190701	5.29	-2.66	5.32	-0.25	6.58	1.00	8.30	2.18	3.74	1.64
20190716	5.03	-0.87	4.37	1.34	5.91	0.42	7.33	1.77	3.71	1.73
20190801	4.07	0.86	3.70	1.32	7.16	0.23	8.76	-0.56	4.06	1.93
20190816	4.59	-1.96	3.38	0.94	5.21	0.71	8.32	0.24	3.78	1.69
20190901	4.17	-0.35	3.73	-0.42	6.27	0.58	7.29	-0.06	3.25	1.61
20190916	3.21	-0.36	3.29	-0.62	5.23	0.60	4.25	2.66	3.50	1.31
20191001	3.23	-1.77	6.11	-4.01	2.72	1.77	4.41	3.55	4.97	2.59
20191016	3.51	-1.96	4.68	-2.65	4.17	0.22	3.96	2.70	4.58	2.45
20191101	3.28	-2.14	5.57	-3.40	2.08	0.49	4.11	1.50	4.79	2.61
20191116	3.64	-2.38	8.85	-6.99	2.04	0.13	3.37	2.04	4.86	3.02
20191201	2.93	-1.82	3.84	-2.54	2.50	-0.51	2.52	0.83	5.91	1.94
20191216	3.45	-2.73	7.55	-6.18	3.93	-2.15	3.10	1.45	5.49	1.93
Max	5.29	1.68	8.89	1.69	7.25	5.21	9.70	4.97	6.87	3.95
Min	2.93	-3.44	3.20	-7.24	1.80	-2.15	2.52	-0.56	3.25	1.19
Median	3.95	-1.92	4.66	-1.73	4.42	0.92	5.33	1.95	4.83	2.07



(a) SGLI L3 LST anomaly (2018-2019) (b) MOD11C1 anomaly (2018-2019)
 Figure 5 Anomaly images from 2018 to 2019 data for second half month of July 2019 in Thailand



(a) SGLI L3 LST anomaly (2009-2019) (b) MOD11C1 anomaly (2009-2019)
 Figure 6 Anomaly images from 2009 to 2019 data for second half month of July 2019 in Thailand

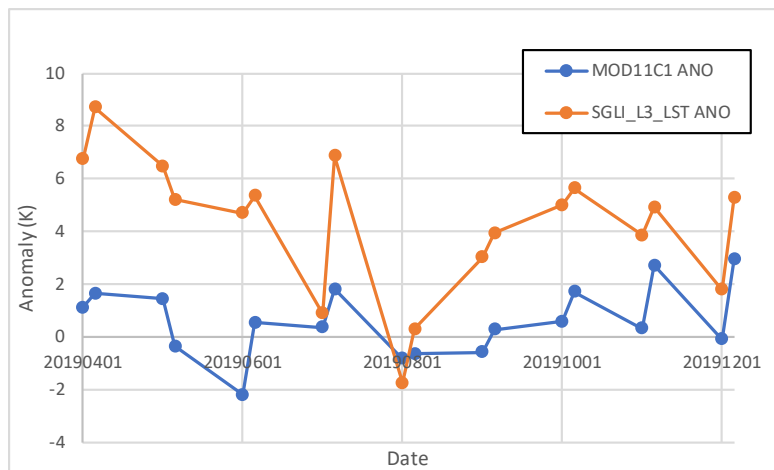


Figure 7 Anomaly time series changes in Thailand, 2019

6. REFERENCES

- FAO, 2009. How to Feed the World in 2050. Rome, Italy, Food and Agriculture Organization. Retrieved October 1, 2020 from http://www.fao.org/fileadmin/templates/wfs/docs/expert_paper/How_to_Feed_the_World_in_2050.pdf.
- Moriyama, M., 2020. GCOM-C1/SGLI Land Surface Temperature Product Algorithm Theoretical Basis Document. Retrieved October 1, 2020 from https://suzaku.eorc.jaxa.jp/GCOM_C/data/ATBD/ver1/LST-ATBD_2014.pdf.
- Sruthi, S., Aslam, M.A.M., 2015. Agricultural Drought Analysis Using the NDVI and Land Surface Temperature

re Data; a Case Study of Raichur District. Aquatic Procedia 4, pp. 1258–1264.
Wan, Z., 2014. New refinements and validation of the collection-6 MODIS land-surface temperature/emissivity product. Remote Sensing of Environment, 140, pp. 36–45.